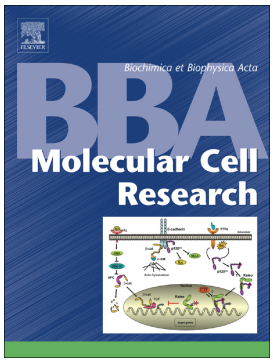

Ubiquitin-dependent proteasomal degradation of AMPK gamma subunit by Cereblon inhibits AMPK activity

Seung-Joo Yang, Seung-Je Jeon, Thang Van Nguyen, Raymond J. Deshaies, Chul-Seung Park, Kwang Min Lee

PII: S0167-4889(20)30087-2

DOI: https://doi.org/10.1016/j.bbamcr.2020.118729

Reference: BBAMCR 118729

To appear in: *BBA - Molecular Cell Research*

Received date: 16 November 2019

Revised date: 12 April 2020

Accepted date: 19 April 2020

Please cite this article as: S.-J. Yang, S.-J. Jeon, T. Van Nguyen, et al., Ubiquitin-dependent proteasomal degradation of AMPK gamma subunit by Cereblon inhibits AMPK activity, *BBA - Molecular Cell Research* (2020), https://doi.org/10.1016/j.bbamcr.2020.118729

Ubiquitin-dependent proteasomal degradation of AMPK gamma subunit by Cereblon inhibits AMPK activity

Seung-Joo Yang[a], Seung-Je Jeon[a], Thang Van Nguyen[b,1], Raymond J. Deshaies[c,2], Chul-Seung Park[a,*], and Kwang Min Lee[d,*]

[a] School of Life Sciences and Aging Research Institute, Gwangju Institute of Science and Technology (GIST), Gwangju 61005, Republic of Korea

[b] Division of Biology and Biological Engineering, California Institute of Technology, Pasadena, CA, USA

[c] Division of Biology and Biological Engineering, and Howard Hughes Medical Institute, California Institute of Technology, Box 114-96, Pasadena, CA 91125, USA

[d] Department of Life Science and Environmental Biochemistry, Pusan National University, Miryang 50463, Republic of Korea

[1] Present address: Department of Medicine, University of Missouri, Columbia, Missouri, USA

[2] Present address: Amgen, One Amgen Center Drive, MS 29-M-B, Thousand Oaks, CA 91320, USA

[*] Correspondence should be addressed to either of the following: Dr. Chul-Seung Park, School of Life Sciences and Aging Research Institute, Gwangju Institute of Science and Technology (GIST), Gwangju 61005, Republic of Korea, E-mail address: cspark@gist.ac.kr; Dr. Kwang Min Lee, Pusan National University, Miryang 50463, Republic of Korea, E-mail address: leekm@pusan.ac.kr

Abstract

Cereblon (CRBN), a substrate receptor for Cullin-ring E3 ubiquitin ligase (CRL), is a major target protein of immunomodulatory drugs. An earlier study demonstrated that CRBN directly interacts with the catalytic α subunit of AMP-activated protein kinase (AMPK), a master regulator of energy homeostasis, down-regulating the enzymatic activity of AMPK. However, it is not clear how CRBN modulates AMPK activity. To investigate the mechanism of CRBN-dependent AMPK inhibition, we measured protein levels of each AMPK subunit in brains, livers, lungs, hearts, spleens, skeletal muscles, testes, kidneys, and embryonic fibroblasts from wild-type and *Crbn*$^{-/-}$ mice. Protein levels and stability of the regulatory AMPKγ subunit were increased in *Crbn*$^{-/-}$ mice. Increased stability of AMPKγ in *Crbn*$^{-/-}$ MEFs was dramatically reduced by exogenous expression of *Crbn*. In wild-type MEFs, the proteasomal inhibitor MG132 blocked degradation of AMPKγ. We also found that CRL4^{CRBN} directly ubiquitinated AMPKγ. Taken together, these findings suggest that CRL4^{CRBN} regulates AMPK through ubiquitin-dependent proteasomal degradation of AMPKγ.

Keywords:

Cereblon; AMP-activated protein kinase γ; ubiquitination; proteasomal degradation

1. Introduction

Cereblon (CRBN), initially identified as a target gene of human intellectual disability [1], is a substrate receptor for the Cullin-4A/B RING E3 ubiquitin ligase (CRL4A) comprising Cullin-4A/B, Damage-specific DNA-binding protein 1 (DDB1), and RING-box protein 1 (ROC1) [2, 3]. $CRL4A^{CRBN}$ mediates the ubiquitination and proteasomal degradation of endogenous substrates such as Ca^{2+}- and voltage-activated K^+ (BK) channels [4, 5], Meis homeobox 2 (MEIS2) [6], CLC-1 chloride [7, 8], and glutamine synthetase (GS) [9]. CRBN was also reported as a primary target protein of immunomodulatory drugs, including thalidomide [3] and its derivatives lenalidomide and pomalidomide [10]. Thalidomide was originally prescribed as a sedative for pregnant women to prevent morning sickness and found to be a teratogen, but thalidomide and its derivatives are now widely used in the treatment of hematologic malignancies such as multiple myeloma [11, 12] and 5q deletion-associated myelodysplastic syndrome [13]. Thalidomide binds CRBN and inhibits $CRL4^{CRBN}$ activity, leading to a teratogenic effect on fetal development [3]. Immunomodulatory drugs bind to CRBN and change its substrate specificity, promoting recruitment of neosubstrates, including Ikaros (IKZF1), Aiolos (IKZF3) [14, 15], and Casein kinase 1A1 (CK1a) [16], leading to their ubiquitin-dependent degradation. Degradation of IKZF1 and IKZF3, which are essential transcription factors in multiple myeloma, results in the death of malignant cells.

AMPK is a master metabolic sensor and regulator of energy homeostasis [17]. AMPK is a heteromeric complex composed of a catalytic α subunit and two regulatory β and γ subunits [18]. The catalytic α subunits contain conventional serine/threonine kinase domains, which are phosphorylated by upstream kinases such as liver kinase B1 (LKB1) [19]. The β subunit contains a carbohydrate-binding module, which allows AMPK to associate with glycogen. The carboxy-terminal domain of the β subunit interacts with both the α and γ subunits, serving as a scaffolding protein. The γ subunit includes four tandem repeats of the Cystathionine β-synthase domain, which are involved in binding adenine nucleotides [20, 21]. Binding of AMP or ADP to the γ subunit leads to a conformational

change that promotes phosphorylation of the α subunit at Thr172 by upstream kinases, as well as protection against dephosphorylation [22, 23 24]. When activated, AMPK phosphorylates various downstream substrates, promoting deactivation of ATP-consuming anabolic pathways and activation of ATP-generating catabolic pathways [25, 26].

Previously, we identified that CRBN inhibits AMPK activity through direct binding to its α subunit *in vitro* and *in vivo*, and that CRBN binding reduces the content of the γ subunit specifically in the AMPK complex [27, 28]. However, the molecular mechanism of CRBN-dependent reduction of AMPKγ is not fully understood. In the present study, we identified that the content of AMPKγ in the AMPK complex was decreased by exogenous CRBN. The amount of endogenous AMPKγ and its stability were increased in *Crbn*$^{-/-}$ mice. Further, we demonstrated that CRL4^{CRBN}-dependent ubiquitination can modulate γ subunit content in the AMPK complex. Taken together, our results demonstrate that CRBN inhibition of AMPK activity is due to ubiquitin-dependent degradation of AMPKγ following interaction between CRBN and AMPKα.

2. Materials and methods

2.1 Experimental animals

Male wild-type C57BL/6J and *Crbn*$^{-/-}$ mice [28] were used in this study. Animals were maintained under specific pathogen-free conditions. All experiments were approved by the Animal Care and Use Committee of Gwangju Institute of Science and Technology.

2.2. Plasmid construction and transfection

Rat AMPKγ was inserted into the pFlag-CMV vector (*Flag-Ampkγ*). Generation of plasmid encoding HA-tagged rat *Crbn* (*HA-Crbn*) was described previously [27]. Cells were transfected using either Lipofectamine 2000 (Invitrogen) or FuGENE HD (Promega) according to the manufacturer's protocols.

2.3. Cell culture

Mouse embryonic fibroblasts (MEFs), *Crbn* knockdown H1299 cells, and *Crbn*$^{-/-}$ HEK293T cells were cultured in Dulbecco's modified Eagle's medium (DMEM, Hyclone) with 10% (v/v) fetal bovine serum (FBS, Hyclone). Wild-type and *Crbn*$^{-/-}$ MEFs were isolated from E14.5 embryos born to heterozygous intercrosses and assayed at passages 3–6, as previously described [29].

2.4. Quantitative real-time PCR analysis.

Total RNA was isolated from wild-type and *Crbn*$^{-/-}$ MEFs by TRIzol reagent (Invitrogen), according to the manufacturer's protocol. Complementary DNA (cDNA) was synthesized using CycleScript RT PreMix (Bioneer). mRNA levels were measured using TB Green™ Premix Ex Taq™

(TaKaRa) and Thermal Cycler Dice Real Time System. The following primers were used for amplification. *Crbn*, forward: 5' AGC ATG GTG CGG AAC TTA ATC-3', and reverse: 5'-ATC TCT GCT GTT GTC CCA AAC-3'; *Ampkα1*, forward: 5'-GTC GAC GTA GCT CCA AGA CC-3', and reverse: 5'-ATC GTT TTC CAG TCC CTG TG-3'; *Ampkβ1*, forward: 5'-GTT GCT GTT GCT TGT TCC AA-3', and reverse: 5'-ATA CTG TGC CTG CCT CTG CT-3'; *Ampkγ1*, forward: 5'-TCC CTA GAC CTC ACC ACA CC-3', and reverse: 5'-GTC TGC ACA GCA CAA GAA CC-3'; 18s rRNA, forward: 5'-GTA ACC CGT TGA ACC CCA TT-3', and reverse: 5'-CCA TCC AAT CGG TAG TAG CG-3'. Expression was normalized to 18s rRNA levels.

2.5. Tissue lysate preparation

Brains, livers, lungs, hearts, spleens, skeletal muscles, testes, and kidneys were isolated from 8-week-old mice. Tissues were homogenized in ice-chilled buffer (20 mM Tris-HCL, pH 7.4, 0.32 M sucrose, 1 mM EDTA, 1 mM EGTA, 1 mM PMSF, 10 μg/ml aprotinin, 15 μg/ml leupeptin, 50 mM NAF, and 1 mM sodium orthovanadate).

2.6. Western blot analysis

Proteins were separated by SDS-PAGE and transferred to polyvinylidene fluoride (PVDF) membranes. After blocking with 3% BSA in TBS-T (137 mM NaCl, 20 mM Tris-Cl, pH 7.6, 0.1% Tween 20), membranes were incubated with various primary antibodies, including rabbit polyclonal anti-CRBN (Sigma), mouse monoclonal anti-AMPKα (Invitrogen), rabbit polyclonal anti-AMPKβ (Cell Signaling), rabbit polyclonal anti-AMPKγ1 (Abcam), rabbit polyclonal anti-β-actin (Sigma), rabbit polyclonal anti-GAPDH (Abfrontier), monoclonal anti-HA (Cell Signaling), monoclonal anti-α-tubulin (Sigma), rabbit polyclonal anti-GFP (Abcam), and monoclonal anti-Flag (Sigma). The blots

were then incubated with horseradish peroxidase (HRP)-conjugated anti-rabbit or mouse secondary antibody (Jackson ImmunoResearch), and developed using enhanced chemiluminescence detection (ECL; Amersham Pharmacia).

2.7. Cycloheximide and MG132 chase experiments

Wild-type and *Crbn*$^{-/-}$ MEFs were seeded overnight in six-well plates, and then treated with 25 μg/ml cycloheximide (ChX; Sigma) or MG132 (Calbiochem) for the indicated times. Treated cells were harvested for Western blot analysis.

2.8. In vivo ubiquitination

H1299 cells stably expressing control shRNA or *Crbn* shRNA were transiently transfected with *Flag-Ampkγ* and *HA-Ub* for 30 hr, and then treated with MG132 (10 μM) for 3 hr. Cells were then lysed using 0.3 ml denaturing IP lysis buffer (1% SDS, 50 mM Tris-HCL, 10 mM DTT, pH 7.5) and boiled for 5 minutes. Denatured proteins were diluted in immunoprecipitation buffer (10 mM Tris-HCl, 150 mM NaCl, 0.5% NP-40, pH 7.6) and immunoprecipitated with anti-Flag resin. Immunoprecipitated proteins were measured by Western blot analysis.

2.9. In vitro ubiquitination

An *in vitro* ubiquitination assay was performed as described previously [30, 31]. Briefly, HEK293T cells were transiently transfected with *Flag-Ampkγ* or empty vector. After 30 hr of transfection, cells were treated with Bortezomib (1μM) for 6 hr. Cell were then lysed in IP buffer and immunoprecipitated with Flag M2 agarose beads for 3 hr. After washing with IP buffer and ubiquitination buffer (50 mM Tris-HCl, pH 8.0, 10 mM $MgCl_2$, 0.2 mM $CaCl_2$, 1 mM DTT, 100 nM

MG132), the beads were incubated at 30°C for 1 hr in 30 μl ubiquitination buffer containing E1 (0.5 μM), UbcH5a (0.5 μM), UbcH3 (1.67 μM), ubiquitin (60 μM), ATP (4 mM), recombinant CUL4A-RBX1, and DDB1-CRBN (250 μM) purified from insect cells. The samples were subjected to Western blot analysis.

2.10. Statistical analysis

All displayed values represent means ± SEM. Significant differences between groups were determined using two-tailed unpaired Student's t-test, and multiple comparisons were performed using one-way ANOVA. Differences with $p < 0.05$ were considered statistically significant, and are indicated in the figure legends.

3. Results

3.1. Protein levels of AMPKγ were specifically increased in Crbn$^{-/-}$ mice

To investigate the regulatory mechanism of AMPK activity by CRBN, we first analyzed endogenous protein levels of AMPK subunits in wild-type and *Crbn*$^{-/-}$ MEFs. AMPKγ protein levels were higher in *Crbn*$^{-/-}$ MEFs than in the wild type (Fig 1A-D). Next, we examined the endogenous protein levels of AMPK α, β, and γ subunits in various tissues of *Crbn*$^{-/-}$ mice. Protein levels of AMPKγ, but not AMPKα or AMPKβ, were increased in the kidney, heart, liver spleen and skeletal muscle of *Crbn*$^{-/-}$ mice (Fig 1E). We then compared the mRNA levels of each AMPK subunit in wild-type and *Crbn*$^{-/-}$ MEFs. No significant differences were observed in the mRNA expression levels of each subunit (Fig 1F-I). These results suggest that CRBN-dependent reduction of AMPKγ was likely post-translational.

3.2. CRBN promoted AMPKγ degradation.

We then evaluated the effect of CRBN on stability of the AMPK α, β, and γ subunits. To determine if the degradation rate of each AMPK subunit was altered by *Crbn* deletion, we treated wild-type and *Crbn*$^{-/-}$ MEFs with cycloheximide (ChX), a protein synthesis inhibitor. MEFs were harvested at different time points (0, 1, 3, 6, and 9 hr) after ChX treatment, and protein levels were measured using Western blot analysis (Fig 2A). No significant differences in protein levels of AMPKα or AMPKβ were detected between cells treated with ChX at all time points tested (Fig 2B and 2D). Contrastingly, protein levels of AMPKγ were increased significantly at the initial time point of ChX treatment, and degraded much more slowly in *Crbn*$^{-/-}$ MEFs relative to wild-type (Fig 2E). While AMPKγ protein level decreased steadily in wild-type MEFs, AMPKγ remained stable up to 9 hr after the initial reduction in *Crbn*$^{-/-}$ MEFs (Fig 2E). The amount of phosphorylated (P-) AMPKα was higher in *Crbn*$^{-/-}$ compared with wild-type at all time-points tested (Fig 2C). Moreover, we compared the mRNA levels of each AMPK subunits in wild-type and *Crbn*$^{-/-}$ MEFs. No significant differences were observed in the mRNA expression levels of each subunit (Fig 2G-I).

To confirm the degradation rate of AMPK subunits by *Crbn* deletion, the effect of *Crbn* knockdown using TD-165, a well characterized CRBN degrader [32], on stability of AMPK subunits was also examined (Fig 3A). Protein levels of AMPKα and AMPKβ were decreased at similar rates in DMSO-treated and TD-165-treated wild-type MEFs (Fig 3B and 3D), while protein levels of AMPKγ were decreased much more slowly in TD-165-treated relative to DMSO-treated wild-type MEFs (Fig 3E).

To investigate the effect of exogenous CRBN on the stability of AMPK subunits, we transiently transfected *Crbn*$^{-/-}$ MEFs with *HA-Crbn* or control plasmid. One day after transfection, we treated the cells with ChX and measured protein levels of AMPK subunits by Western blot analysis at various time points (Fig 4A). In the absence of exogenous CRBN, AMPKγ was relatively stable, with more than 50% of AMPKγ remaining after 9 hr ChX treatment. However, AMPKγ was dramatically

decreased by ectopic expression of *Crbn*, with a half-life of less than 3 hr (Fig 4E). Protein levels of P-AMPK were lower in the presence of exogenous CRBN (Fig 4C). However, there was no difference in the mRNA levels of AMPK subunits between the groups (Fig 4F-H). Exogenous CRBN did not affect the degradation rates of AMPKα or AMPKβ (Fig 4B and 4D). These results indicated that CRBN accelerated the degradation of AMPKγ, but not AMPKα or AMPKβ.

3.3 CRBN regulated AMPKγ in a proteasome-dependent manner.

Because CRBN functions as the substrate receptor of CRL4 E3 ubiquitin ligase and recruits specific target proteins for degradation through the ubiquitin proteasome pathway, we surmised that CRBN reduction of AMPKγ protein level could be due to proteasomal degradation. We assessed the accumulation rates of AMPK subunits in wild-type and *Crbn*$^{-/-}$ MEFs. Cells were treated with MG132 for 0, 1, 3, 6, and 9 hr to inhibit proteasome activity. We than examined protein levels of AMPKα, β, and γ by Western blot analysis (Fig 5A). AMPKα and AMPKβ accumulated at similar rates in wild-type and *Crbn*$^{-/-}$ MEFs (Fig. 5B and D), while AMPKγ accumulated at a much faster rate in wild-type MEFs (Fig. 5E). After a 9 hr treatment with MG132, AMPKγ, which was initially lower in wild-type MEFs relative to *Crbn*$^{-/-}$ MEFs, increased to similar levels as that of *Crbn*$^{-/-}$ MEFs (Fig 5E). P-AMPKα accumulated more rapidly in wild-type MEFs (Fig 5C). There were no statistical differences in the mRNA expression levels of each AMPK subunit between cells (Fig 5G-I). MG132 preservation of AMPKγ against CRBN-dependent degradation strongly suggested that CRBN degradation of AMPK was modulated by the ubiquitin proteasome.

3.4. Ubiquitination of AMPKγ was mediated by CRL4^{CRBN}.

Because *Crbn* knockout increased AMPKγ protein stability without affecting mRNA levels, we further investigated whether AMPKγ was a substrate of CRBN. To determine whether AMPKγ was ubiquitinated by CRL4^{CRBN}, we co-expressed Flag-tagged AMPKγ (*Flag-Ampkγ*) and HA-tagged

ubiquitin (*HA-Ub*) in H1299 cells stably expressing control or *Crbn* shRNA. After 30 hr of transfection, cells were treated with MG132 to stabilize ubiquitinated proteins, and Flag-AMPKγ was immunoprecipitated. Subsequent Western blot analysis with HA antibodies to detect ubiquitinated proteins revealed a high-molecular weight smear of Flag-AMPKγ. In addition, *Crbn* knockdown decreased AMPKγ ubiquitination (Fig 6A).

Next, we performed an *in vitro* ubiquitination assay to investigate whether $CRL4^{CRBN}$ directly ubiquitinated AMPKγ. We purified Flag-tagged AMPKγ, CUL4A-RBX1, and DDB1-CRBN. The reactions were analyzed by Western blotting using anti-Flag antibody to detect a high-molecular weight smear of Flag-AMPKγ. *In vitro* ubiquitination of Flag-AMPKγ was markedly increased after supplemental addition of E1, E2, ubiquitin, and $CRL4^{CRBN}$, and was inhibited by methylated ubiquitin (Me-Ub) (Fig 6B). Taken together, these results suggest that $CRL4^{CRBN}$ promoted AMPKγ ubiquitination.

4. Conclusions

AMPK, which consists of a catalytic α subunit and regulatory β and γ subunits, is a highly conserved master regulator of metabolism, the activity of which is regulated by cellular AMP/ATP and ADP/ATP ratios [17, 18]. Among the AMPK subunits, the regulatory γ subunits contain four tandem repeats of CBS domains responsible for adenine nucleotide binding (AMP, ADP, or ATP), allowing AMPK to sense cellular energy status [20, 21, 22, 23]. Further, several mutations in the γ subunit lead to changes in AMPK activity and sensitivity to AMP [33, 34].

Previously, we reported that CRBN negatively modulates AMPK activity via direct binding to AMPKα, and that this binding decreases the level of AMPKγ in the AMPK complex [27]. Subsequently, we demonstrated that AMPK activity was constitutively activated in *Crbn* knockout mice under normal conditions and that *Crbn* knockout mice fed a long-term high-fat diet (HFD) showed a noticeable improvement in their metabolic status [28]. In the present study, we focused on the molecular mechanism of CRBN-mediated AMPK inhibition, and demonstrated that ubiquitin-dependent proteasomal degradation of AMPKγ by $CRL4^{CRBN}$ suppressed AMPK.

First, we measured the endogenous protein levels of AMPK subunits in the absence and presence of the *Crbn* gene (Fig. 1). In $Crbn^{-/-}$ MEFs, protein levels of endogenous γ subunits, but not α or β subunits, were increased. Because no significant differences were observed in γ subunit mRNA levels between wild-type and $Crbn^{-/-}$ MEFs, the decreased protein level of AMPKγ was likely due to post-translational processes. We next compared AMPK subunit protein levels in various tissues from wild-type and $Crbn^{-/-}$ mice, and observed similar increases of AMPKγ in several $Crbn^{-/-}$ tissues, most notably in the kidney, liver, heart, and spleen (Fig 1E). The tissue-specific effects of *Crbn* knockout were not simply due to the abundance of CRBN in specific tissues *per se*, and thus tissue-specific CRBN modulation of AMPKγ is a topic of future investigation.

Because CRBN recruits its target proteins for ubiquitination, we examined the protein stability of AMPKγ under inhibition of protein synthesis and imbibition of proteasomal degradation.

When *de novo* protein synthesis was blocked, AMPKγ was degraded more slowly in the absence of CRBN, while AMPKα and AMPKβ were unaffected by CRBN (Fig 2 and 3). Further, AMPKγ degradation was facilitated by the presence of exogenous CRBN (Fig 4). Furthermore, in the presence of a proteasomal inhibitor, only AMPKγ accumulated more rapidly in wild-type MEFs than in *Crbn*$^{-/-}$ MEFs (Fig 5). Moreover, no significant differences in mRNA levels of AMPK subunits were observed between cells treated ChX or MG132 at all time points (Fig 2, 4 and 5). These results strongly suggested CRBN-dependent ubiquitination and subsequent degradation of AMPKγ via the ubiquitin-proteasome pathway. This was validated by an *in vitro* ubiquitination assay of AMPKγ (Fig 6).

Control of AMPK phosphorylation by upstream kinases and phosphatases is the most characterized mechanism of AMPK regulation. However, several recent studies identified that post-translational modification of AMPK levels through ubiquitination also regulates AMPK activity [35]. AMPKα is ubiquitinated by UBE2O, an E2 ubiquitin-conjugating enzyme, and subsequently targeted for proteasomal degradation [36]. Tripartite motif-containing 28 (TRIM28) [37] and Makorin ring finger protein 1 (MKRN1), an E3 ubiquitin ligase [38], also regulate AMPKα ubiquitination and proteasomal degradation. In brown adipose tissue, Cell death-inducing DFFA-like effector a (Cidea) ubiquitinates and degrades AMPKβ [39]. However, this is the first report to identify ubiquitination of the AMPKγ subunit.

The experimental results of this study, together with previous findings [27, 28], suggest that CRBN may interact with the α subunit of AMPK as a trimeric complex, and that $CRL4^{CRBN}$ may transfer ubiquitin to specific site(s) in the γ subunit for subsequent proteasomal degradation. Thus, the present study identifies a novel mechanism for regulation of AMPK activity through $CRL4^{CRBN}$-dependent degradation of AMPKγ, and provides a plausible explanation for the HFD-induced metabolic disorder-resistant phenotype observed in *Crbn*$^{-/-}$ mice [28].

Acknowledgments

We thank Dr. Jong Yeon Kwang (Korea Research Institute of Chemical Technology) for kindly providing us with the TD-165. This work was supported by grants for the Korea Healthcare Technology Research and Development Project (HI13C1412), Ministry for Health and Welfare, GIST Research Institute (GRI), funded by the GIST in 2019, and Cell Logistics Research Center, National Research Foundation of Korea (NRF-2016R1A5A1007318).

Conflicts of interest

The authors have no competing financial interests related to the work presented in this manuscript.

Author contributions

Seung-Joo Yang: Investigation, Validation, Formal analysis, and Writing – Original Draft, Seung-Je Jeon: Investigation and Validation, Thang Van Nguyen: Investigation and Validation, Raymond J. Deshaies: Investigation, and Review & Editing, Chul-Seung Park: Conceptualization, Writing – Review & Editing, and Supervision, Kwang Min Lee: Conceptualization, Investigation, Validation, Writing – Review & Editing, and Supervision.

Figure 1: Protein and mRNA levels of AMPK subunits in wild-type and *Crbn*$^{-/-}$ MEFs and somatic tissues.

(A) Wild-type and *Crbn*$^{-/-}$ MEF lysates were subjected to Western blot analysis with the indicated antibodies. Glyceraldehyde-3-phosphate dehydrogenase (GAPDH) was used as a loading control, and ratios of **(B)** AMPKα, **(C)** AMPKβ, and **(D)** AMPKγ1 to GAPDH were calculated. **(E)** Proteins extracted from various tissues (brain, liver, lung, heart, spleen, skeletal muscle, testis, and kidney) of wild-type and *Crbn*$^{-/-}$ mice were separated by SDS-PAGE and immunoblotted with anti-AMPKα, anti-AMPKβ, anti-AMPKγ, and anti-β-actin antibodies. Eight-week-old male mice were used. **(F-I)** Total RNA was isolated from wild-type and *Crbn*$^{-/-}$ MEFs, and subjected to quantitative real-time PCR analysis to determine the expression of (F) *Crbn*, (G) *Ampkα*, (H) *Ampkβ*, and (I) *Ampkγ*. Expression was normalized against 18s rRNA levels. # and ## indicate AMPKβ isoform 1 and 2, respectively. Error bars represent the SEM (n=6). *P < 0.05, **P < 0.01, ***P < 0.005, ****P < 0.001.

Figure 2: Increased stability of AMPKγ in *Crbn*$^{-/-}$ MEFs.

Wild-type and *Crbn*$^{-/-}$ MEFs were treated with ChX (25 μg/ml) for the specified times. Cell lysates were analyzed by Western blot. **(A)** Representative Western blots of endogenous AMPKα, P-AMPKα, AMPKβ, AMPKγ1, CRBN, and α-tubulin. α-Tubulin was used as a loading control. **(B-F)** Western blotting results in (A) were quantified by densitometry and values were plotted. Relative mRNA levels of (G) *Ampkα*, (H) *Ampkβ*, and (I) *Ampkγ*. Expression was normalized against 18s rRNA levels. A single-exponential decay curve was fit. Error bars represent the SEM (n=4). Empty circles indicate individual values of protein or mRNA level. Filled circles indicate mean values of protein or mRNA level. *P < 0.05, **P < 0.01, ***P < 0.005, ****P < 0.001 vs. wild-type MEFs untreated with ChX. †P < 0.05, ††P < 0.01, †††P < 0.005, ††††P < 0.001 vs. *Crbn*$^{-/-}$ MEFs untreated with ChX. §P < 0.05, §§P < 0.01, §§§P < 0.005, §§§§P < 0.001 vs. wild-type MEFs at the same ChX

treatment time point.

Figure 3: Increased stability of AMPKγ by CRBN knockdown

Wild-type MEFs were treated with TD-165 (0.5 μM). After 24 hr, cells were treated with ChX (25 ug/ml) for the indicated times. Cell lysates were analyzed by Western blot. **(A)** Representative Western blots of endogenous AMPKα, P-AMPKα, AMPKβ, AMPKγ1, CRBN, and α-tubulin. α-Tubulin was used as a loading control. **(B-F)** Western blotting results in (A) were quantified by densitometry and values were plotted. # indicate CRBN. A single-exponential decay curve was fit. Error bars represent the SEM (n=4). Empty circles indicate individual values of protein level. Filled circles indicate mean values of protein levels. *P < 0.05, **P < 0.01, ***P < 0.005, ****P < 0.001 vs. wild-type MEFs untreated with ChX. †P < 0.05, ††P < 0.01, †††P < 0.005, ††††P < 0.001 vs. *Crbn*$^{-/-}$ MEFs untreated with ChX. §P < 0.05, §§P < 0.01, §§§P < 0.005, §§§§P < 0.001 vs. wild-type MEFs at the same ChX treatment time point.

Figure 4: Exogenous CRBN accelerated AMPKγ degradation.

Crbn$^{-/-}$ MEFs were transiently transfected with *pcDna3-HA* or *pcDna3-HA/Crbn* (*HA-Crbn*). After 24 hr, cells were treated with ChX (25 μg/ml) for the indicated times. **(A)** Cell lysates were subjected to Western blot analysis for AMPKα, P-AMPKα, AMPKβ, AMPKγ1, α-tubulin, HA, and GFP. GFP was used as a marker for transfection efficiency and α-tubulin was used as a loading control. **(B-E)** The results in (A) were quantified and normalized against α-tubulin levels, and values were plotted. Relative mRNA levels of (F) *Ampkα*, (G) *Ampkβ*, and (H) *Ampkγ*. Expression was normalized against 18s rRNA levels. A single-exponential decay curve was fit. Error bars represent the SEM (n=4). Empty circles indicate individual values of protein or mRNA level. Filled circles indicate mean values

of protein or mRNA levels. *P < 0.05, **P < 0.01, ***P < 0.005, ****P < 0.001 vs. wild-type MEFs untreated with ChX. †P < 0.05, ††P < 0.01, †††P < 0.005, ††††P < 0.001 vs. *Crbn*$^{-/-}$ MEFs untreated with ChX. §P < 0.05, §§P < 0.01, §§§P < 0.005, §§§§P < 0.001 vs. wild-type MEFs at the same ChX treatment time point.

Figure 5: Proteasomal inhibition prevented CRBN-mediated AMPKγ degradation.

Wild-type and *Crbn*$^{-/-}$ MEFs were treated with MG132 (0.5 μM) for the indicated times. Cell lysates were analyzed by Western blot. **(A)** Representative Western blots of endogenous AMPKα, P-AMPKα, AMPKβ, AMPKγ1, CRBN, and α-tubulin. α-Tubulin was used as a loading control. **(B-F)** The results in (A) were quantified by densitometry and normalized to α-tubulin, and values were plotted. Relative mRNA levels of (G) *Ampkα*, (H) *Ampkβ*, and (I) *Ampkγ*. Expression was normalized against 18s rRNA levels. A single-exponential growth curve was fitted. Error bars represent the SEM (n=4). Empty circles indicate individual values of protein or mRNA level. Filled circles indicate mean values of protein or mRNA levels. *P < 0.05, **P < 0.01, ***P < 0.005, ****P < 0.001 vs. wild-type MEFs untreated with MG132. †P < 0.05, ††P < 0.01, †††P < 0.005, ††††P < 0.001 vs. *Crbn*$^{-/-}$ MEFs untreated with MG132. §P < 0.05, §§P < 0.01, §§§P < 0.005, §§§§P < 0.001 vs. wild-type MEFs at the same MG132 treatment time point.

Figure 6: CRL4^{CRBN} regulated AMPKγ ubiquitination.

(A) H1299 cells stably expressing control (CT) or *Crbn* shRNA were transiently transfected with *Flag-Ampk* and *HA-ubiquitin* (Ub). After 30 hr of transfection, cells were treated with MG132 (10 μM) for 3 hr. Cell lysates were immunoprecipitated with `anti-Flag resin under denaturing conditions. The input and immunoprecipitated fractions were detected by Western blotting for HA and Flag. LC

indicates the IgG light chain. Numerical band intensity (mean ± SEM) was measured by NIH image J and indicated figure. **(B)** Flag-AMPKγ was purified from *Crbn*$^{-/-}$ 293FT cells. An *in vitro* ubiquitination assay of Flag-AMPKγ was performed in the presence or absence of E1 + E2 and HA-Ub. Where indicated, methylated Ub (Me-Ub) or recombinant CUL4A^{CRBN} purified from insect cells was added. (Ub)n indicates polyubiquitination.

References

[1] J.J. Higgins, J. Pucilowska, R.Q. Lombardi, J.P.J.N. Rooney, A mutation in a novel ATP-dependent Lon protease gene in a kindred with mild mental retardation, Neurology. 63 (2004) 1927-1931.

[2] S. Angers, T. Li, X. Yi, M.J. MacCoss, R.T. Moon, N.J.N. Zheng, Molecular architecture and assembly of the DDB1–CUL4A ubiquitin ligase machinery, Nature. 443 (2006) 590.

[3] T. Ito, H. Ando, T. Suzuki, T. Ogura, K. Hotta, Y. Imamura, Y. Yamaguchi, H.J.s. Handa, Identification of a primary target of thalidomide teratogenicity, Science. 327 (2010) 1345-1350.

[4] S. Jo, K.H. Lee, S. Song, Y.K. Jung, C.S.J.J.o.n. Park, Identification and functional characterization of cereblon as a binding protein for large-conductance calcium-activated potassium channel in rat brain, J Neurochem. 94 (2005) 1212-1224.

[5] J. Liu, J. Ye, X. Zou, Z. Xu, Y. Feng, X. Zou, Z. Chen, Y. Li, Y.J.N.c. Cang, CRL4A CRBN E3 ubiquitin ligase restricts BK channel activity and prevents epileptogenesis, Nat Commun. 5 (2014) 3924.

[6] E.S. Fischer, K. Böhm, J.R. Lydeard, H. Yang, M.B. Stadler, S. Cavadini, J. Nagel, F. Serluca, V. Acker, G.M.J.N. Lingaraju, Structure of the DDB1–CRBN E3 ubiquitin ligase in complex with thalidomide, Nature. 512 (2014) 49.

[7] B. Hohberger, R.J.F.l. Enz, Cereblon is expressed in the retina and binds to voltage- gated chloride channels, FEBS Lett. 583 (2009) 633-637.

[8] Y.-A. Chen, Y.-J. Peng, M.-C. Hu, J.-J. Huang, Y.-C. Chien, J.-T. Wu, T.-Y. Chen, C.-Y.J.S.r. Tang, The cullin 4A/B-DDB1-cereblon E3 ubiquitin ligase complex mediates the degradation of CLC-1 chloride channels, Sci Rep. 5 (2015) 10667.

[9] T. Van Nguyen, J.E. Lee, M.J. Sweredoski, S.-J. Yang, S.-J. Jeon, J.S. Harrison, J.-H. Yim, S.G. Lee, H. Handa, B.J.M.c. Kuhlman, Glutamine triggers acetylation-dependent degradation of glutamine synthetase via the thalidomide receptor cereblon, Mol Cell. 61 (2016) 809-820.

[10] Y.X. Zhu, E. Braggio, C.-X. Shi, L.A. Bruins, J.E. Schmidt, S. Van Wier, X.-B. Chang, C.C. Bjorklund, R. Fonseca, P.L.J.B. Bergsagel, Cereblon expression is required for the antimyeloma

activity of lenalidomide and pomalidomide, Blood. 118 (2011) 4771-4779.

[11] S. Singhal, J. Mehta, R. Desikan, D. Ayers, P. Roberson, P. Eddlemon, N. Munshi, E. Anaissie, C. Wilson, M.J.N.E.J.o.M. Dhodapkar, Antitumor activity of thalidomide in refractory multiple myeloma, N Engl J Med. 341 (1999) 1565-1571.

[12] M.J.B. Cavo, A third-generation IMiD for MM, Blood. 118 (2011) 2931-2932.

[13] B. Pan, S.J.P. Lentzsch, therapeutics, The application and biology of immunomodulatory drugs (IMiDs) in cancer, Pharmacol Ther. 136 (2012) 56-68.

[14] J. Krönke, N.D. Udeshi, A. Narla, P. Grauman, S.N. Hurst, M. McConkey, T. Svinkina, D. Heckl, E. Comer, X.J.S. Li, Lenalidomide causes selective degradation of IKZF1 and IKZF3 in multiple myeloma cells, Science. 343 (2014) 301-305.

[15] G. Lu, R.E. Middleton, H. Sun, M. Naniong, C.J. Ott, C.S. Mitsiades, K.-K. Wong, J.E. Bradner, W.G.J.S. Kaelin, The myeloma drug lenalidomide promotes the cereblon-dependent destruction of Ikaros proteins, Science. 343 (2014) 305-309.

[16] J. Krönke, E.C. Fink, P.W. Hollenbach, K.J. MacBeth, S.N. Hurst, N.D. Udeshi, P.P. Chamberlain, D. Mani, H.W. Man, A.K.J.N. Gandhi, Lenalidomide induces ubiquitination and degradation of CK1α in del (5q) MDS, Nature. 523 (2015) 183.

[17] D.G.J.N.r.M.c.b. Hardie, AMP-activated/SNF1 protein kinases: conserved guardians of cellular energy, Nat Rev Mol Cell Biol. 8 (2007) 774.

[18] J.R. Dyck, G. Gao, J. Widmer, D. Stapleton, C.S. Fernandez, B.E. Kemp, L.A.J.J.o.B.C. Witters, Regulation of 5′-AMP-activated protein kinase activity by the noncatalytic β and γ subunits, J Biol Chem. 271 (1996) 17798-17803.

[19] S.A. Hawley, J. Boudeau, J.L. Reid, K.J. Mustard, L. Udd, T.P. Mäkelä, D.R. Alessi, D.G.J.J.o.b. Hardie, Complexes between the LKB1 tumor suppressor, STRADα/β and MO25α/β are upstream kinases in the AMP-activated protein kinase cascade, J Biol. 2 (2003) 28.

[20] J. Oakhill, J. Scott, B.J.A.p. Kemp, Structure and function of AMP- activated protein kinase, Acta Physiol (Oxf). 196 (2009) 3-14.

[21] B. Xiao, R. Heath, P. Saiu, F.C. Leiper, P. Leone, C. Jing, P.A. Walker, L. Haire, J.F. Eccleston, C.T.J.N. Davis, Structural basis for AMP binding to mammalian AMP-activated protein kinase, Nature. 449 (2007) 496.

[22] B. Xiao, M.J. Sanders, E. Underwood, R. Heath, F.V. Mayer, D. Carmena, C. Jing, P.A. Walker, J.F. Eccleston, L.F.J.N. Haire, Structure of mammalian AMPK and its regulation by ADP, Nature. 472 (2011) 230.

[23] G.J. Gowans, S.A. Hawley, F.A. Ross, D.G.J.C.m. Hardie, AMP is a true physiological regulator of AMP-activated protein kinase by both allosteric activation and enhancing net phosphorylation, Cell Metab. 18 (2013) 556-566.

[24] S.A. Hawley, M. Davison, A. Woods, S.P. Davies, R.K. Beri, D. Carling, D.G.J.J.o.B.C. Hardie, Characterization of the AMP-activated protein kinase kinase from rat liver and identification of threonine 172 as the major site at which it phosphorylates AMP-activated protein kinase, J Biol Chem. 271 (1996) 27879-27887.

[25] G.R. Steinberg, B.E.J.P.r. Kemp, AMPK in health and disease, Physiol Rev. 89 (2009) 1025-1078.

[26] D.J.T.i.b.s. Carling, The AMP-activated protein kinase cascade–a unifying system for energy control, Trends Biochem Sci. 29 (2004) 18-24.

[27] K.M. Lee, S. Jo, H. Kim, J. Lee, C.-S.J.B.e.B.A.-M.C.R. Park, Functional modulation of AMP-activated protein kinase by cereblon, Biochim Biophys Acta. 1813 (2011) 448-455.

[28] K.M. Lee, S.-J. Yang, Y.D. Kim, Y.D. Choi, J.H. Nam, C.S. Choi, H.-S. Choi, C.-S.J.D. Park, Disruption of the cereblon gene enhances hepatic AMPK activity and prevents high-fat diet–induced obesity and insulin resistance in mice, Diabetes. 62 (2013) 1855-1864.

[29] J.J.C.p.i.m.b. Xu, Preparation, culture, and immortalization of mouse embryonic fibroblasts, Curr Protoc Mol Biol. 70 (2005) 28.21. 21-28.21. 28.

[30] S. Duan, L. Cermak, J.K. Pagan, M. Rossi, C. Martinengo, P.F. di Celle, B. Chapuy, M. Shipp, R. Chiarle, M.J.N. Pagano, FBXO11 targets BCL6 for degradation and is inactivated in diffuse large B-cell lymphomas, Nature. 481 (2012) 90.

[31] G. Kleiger, A. Saha, S. Lewis, B. Kuhlman, R.J.J.C. Deshaies, Rapid E2-E3 assembly and disassembly enable processive ubiquitylation of cullin-RING ubiquitin ligase substrates, Cell. 139 (2009) 957-968.

[32] K. Kim, D.H. Lee, S. Park, S.-H. Jo, B. Ku, S.G. Park, B.C. Park, Y.U. Jeon, S. Ahn, C.H.J.S.r. Kang, Disordered region of cereblon is required for efficient degradation by proteolysis-targeting chimera, Sci Rep. 9 (2019) 1-14.

[33] S.R. Hamilton, D. Stapleton, J.B. O'Donnell, J.T. Kung, S.R. Dalal, B.E. Kemp, L.A.J.F.l. Witters, An activating mutation in the γ1 subunit of the AMP- activated protein kinase, FEBS Lett. 500 (2001) 163-168.

[34] J. Adams, Z.P. Chen, B.J. Van Denderen, C.J. Morton, M.W. Parker, L.A. Witters, D. Stapleton, B.E.J.P.s. Kemp, Intrasteric control of AMPK via the γ1 subunit AMP allosteric regulatory site, Protein Sci. 13 (2004) 155-165.

[35] M. Zungu, J.C. Schisler, M.F. Essop, C. McCudden, C. Patterson, M.S.J.T.A.j.o.p. Willis, Regulation of AMPK by the ubiquitin proteasome system, Am J Pathol. 178 (2011) 4-11.

[36] I.K. Vila, Y. Yao, G. Kim, W. Xia, H. Kim, S.-J. Kim, M.-K. Park, J.P. Hwang, E. González-Billalabeitia, M.-C.J.C.C. Hung, A UBE2O-AMPKα2 axis that promotes tumor initiation and progression offers opportunities for therapy, Cancer Cell. 31 (2017) 208-224.

[37] C.T. Pineda, S. Ramanathan, K.F. Tacer, J.L. Weon, M.B. Potts, Y.-H. Ou, M.A. White, P.R.J.C. Potts, Degradation of AMPK by a cancer-specific ubiquitin ligase, Cell. 160 (2015) 715-728.

[38] M.-S. Lee, H.-J. Han, S.Y. Han, I.Y. Kim, S. Chae, C.-S. Lee, S.E. Kim, S.G. Yoon, J.-W. Park, J.-H.J.N.c. Kim, Loss of the E3 ubiquitin ligase MKRN1 represses diet-induced metabolic syndrome through AMPK activation, Nat Commum. (2018) 3404.

[39] J. Qi, J. Gong, T. Zhao, J. Zhao, P. Lam, J. Ye, J.Z. Li, J. Wu, H.M. Zhou, P.J.T.E.j. Li, Downregulation of AMP-activated protein kinase by Cidea-mediated ubiquitination and degradation in brown adipose tissue, EMBO J. 27 (2008) 1537-1548.

Author contributions

Seung-Joo Yang: Investigation, Validation, Formal analysis, and Writing – Original Draft, Seung-Je Jeon: Investigation and Validation, Thang Van Nguyen: Investigation and Validation, Raymond J. Deshaies: Investigation, and Review & Editing, Chul-Seung Park: Conceptualization, Writing – Review & Editing, and Supervision, Kwang Min Lee: Conceptualization, Investigation, Validation, Writing – Review & Editing, and Supervision.

Declaration of interests

☒ The authors declare that they have no known competing financial interests or personal relationships that could have appeared to influence the work reported in this paper.

☐The authors declare the following financial interests/personal relationships which may be considered as potential competing interests:

Highlights

- Ablation of the *Crbn* gene increased protein levels of the AMP-activation protein kinase (AMPK) γ subunit.
- Exogenous CRBN promoted degradation of AMPKγ.
- Proteasomal inhibition attenuated CRBN-dependent AMPKγ degradation.
- AMPKγ was ubiquitinated and degraded by $CRL4^{CRBN}$.

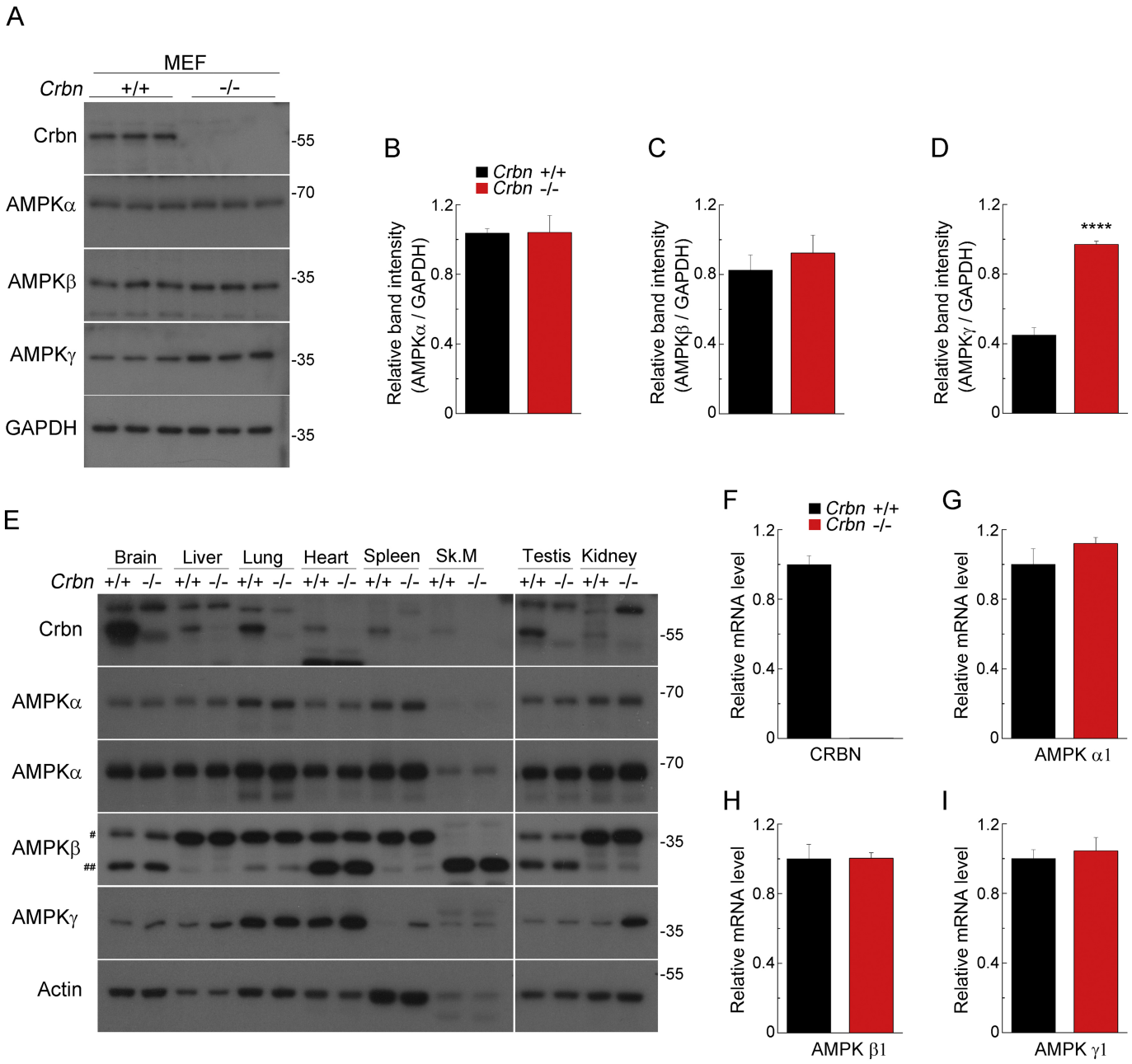
A
MEF
Crbn +/+ -/-
Crbn
AMPKα
AMPKβ
AMPKγ
GAPDH
-55
-70
-35
-35
-35
B
Crbn +/+
Crbn -/-
Relative band intensity (AMPKα / GAPDH)
1.2
0.8
0.4
0
C
Relative band intensity (AMPKβ / GAPDH)
D
Relative band intensity (AMPKγ / GAPDH)
****
E
Brain Liver Lung Heart Spleen Sk.M Testis Kidney
Crbn +/+ -/- +/+ -/- +/+ -/- +/+ -/- +/+ -/- +/+ -/- +/+ -/- +/+ -/-
Crbn
AMPKα
AMPKα
AMPKβ
#
##
AMPKγ
Actin
-55
-70
-70
-35
-35
-55
F
Crbn +/+
Crbn -/-
Relative mRNA level
CRBN
G
AMPK α1
H
AMPK β1
I
AMPK γ1

Figure 1

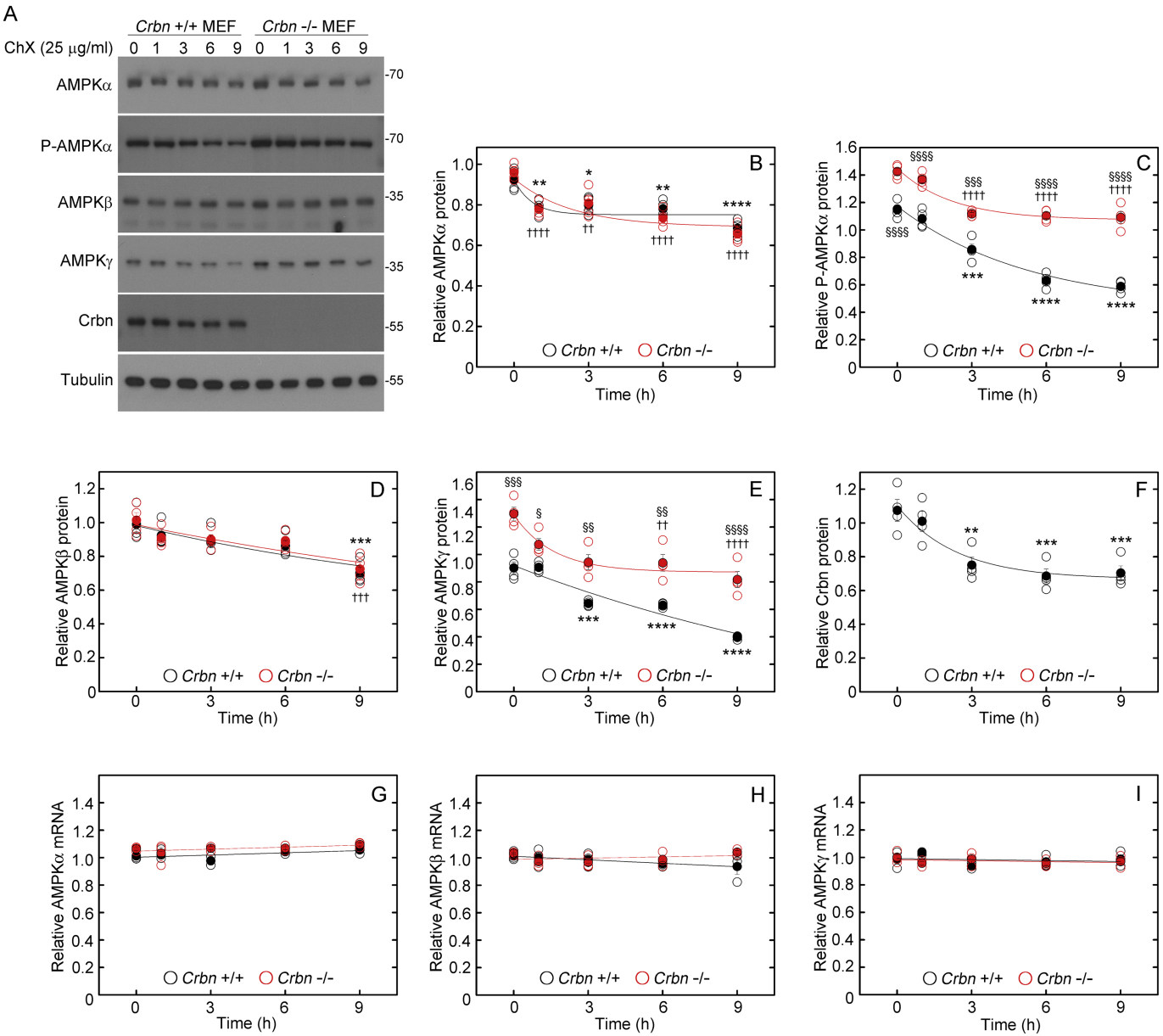
A
Crbn +/+ MEF
Crbn -/- MEF
ChX (25 μg/ml)
0 1 3 6 9 0 1 3 6 9
AMPKα
P-AMPKα
AMPKβ
AMPKγ
Crbn
Tubulin
-70
-70
-35
-35
-55
-55
B
Relative AMPKα protein
C
Relative P-AMPKα protein
D
Relative AMPKβ protein
E
Relative AMPKγ protein
F
Relative Crbn protein
G
Relative AMPKα mRNA
H
Relative AMPKβ mRNA
I
Relative AMPKγ mRNA
Crbn +/+
Crbn -/-
Time (h)

Figure 2

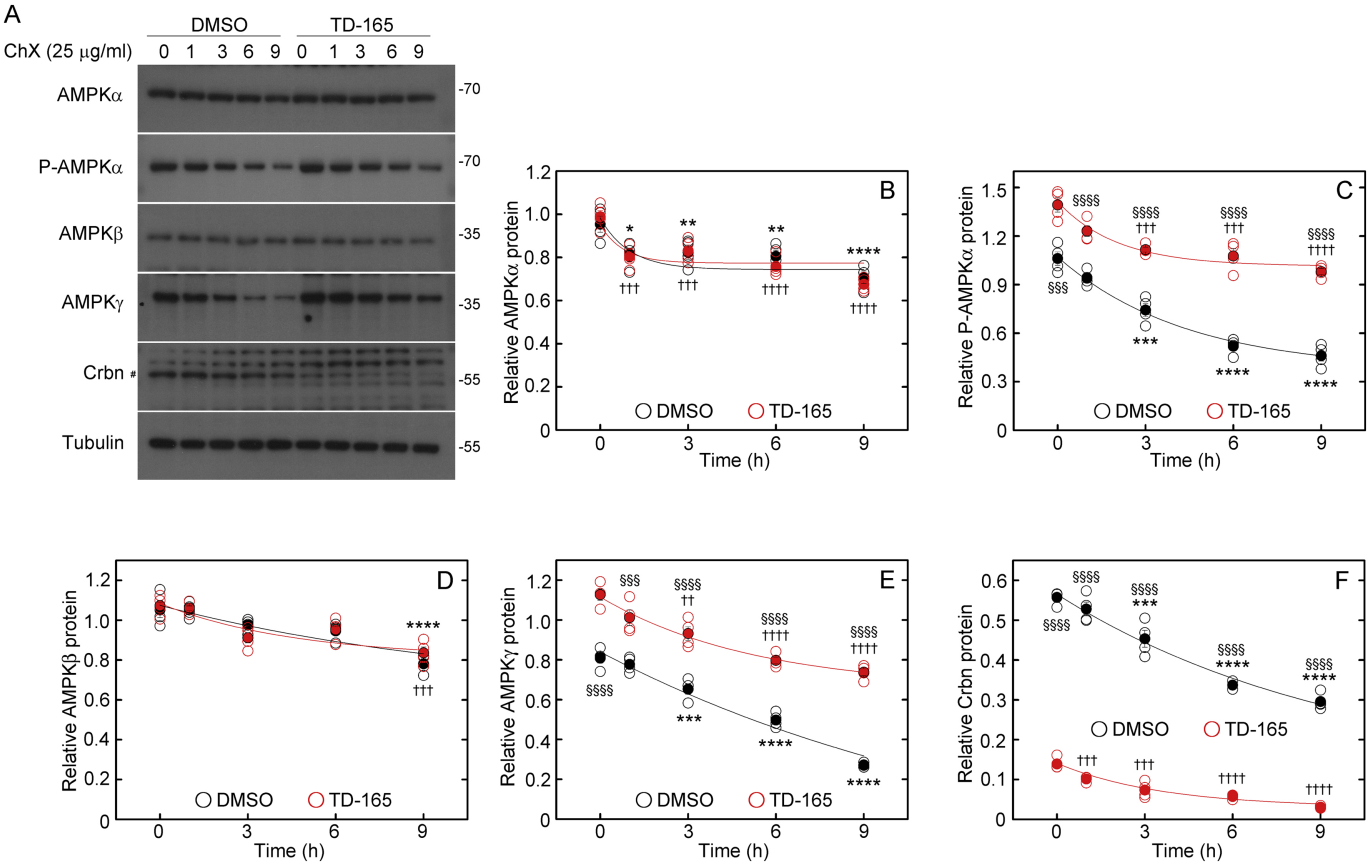
A
DMSO
TD-165
ChX (25 μg/ml)
0 1 3 6 9 0 1 3 6 9
AMPKα
P-AMPKα
AMPKβ
AMPKγ
Crbn #
Tubulin
-70
-70
-35
-35
-55
-55
B
Relative AMPKα protein
Time (h)
DMSO
TD-165
C
Relative P-AMPKα protein
D
Relative AMPKβ protein
E
Relative AMPKγ protein
F
Relative Crbn protein

Figure 3

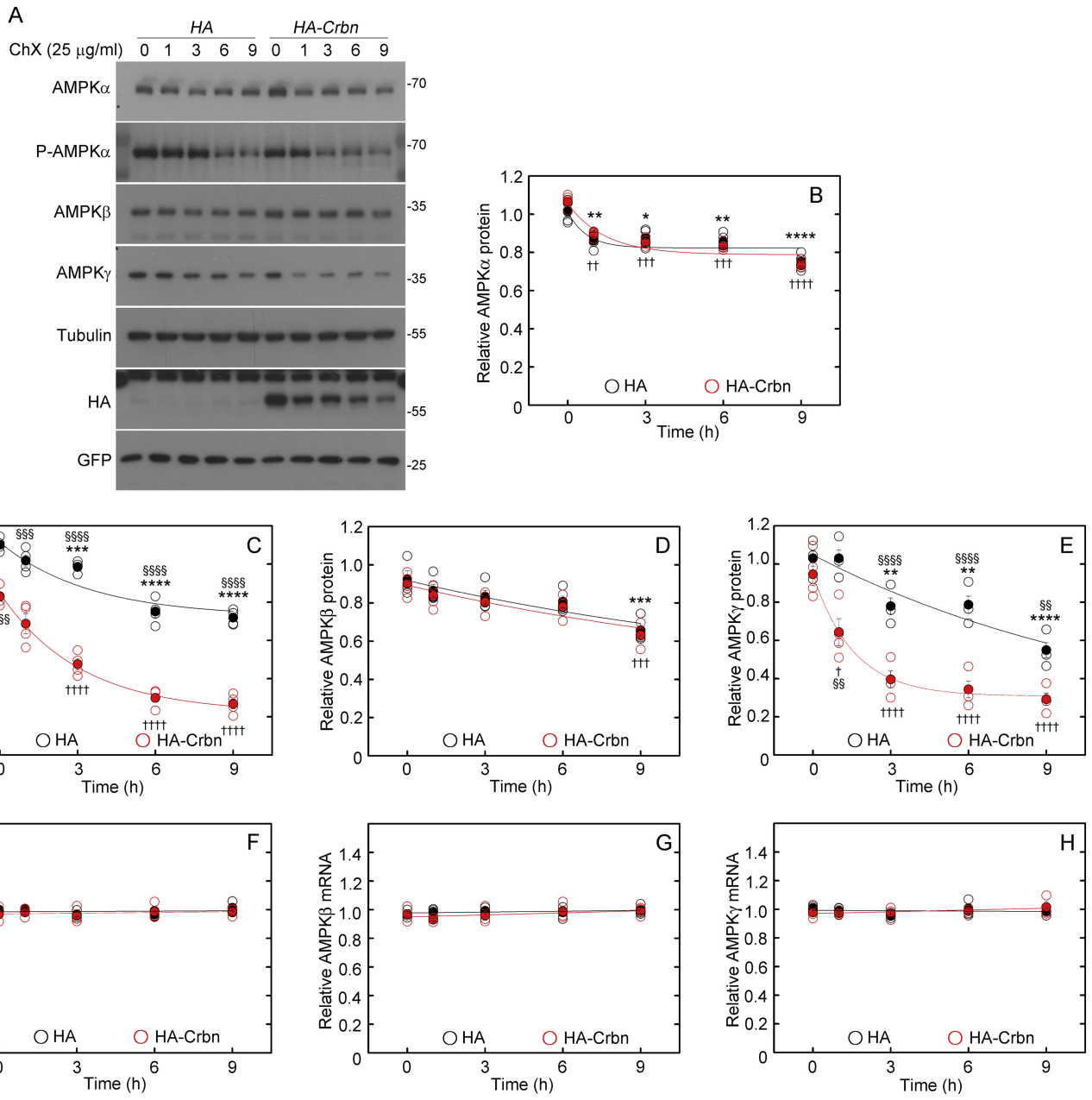
A
HA
HA-Crbn
ChX (25 μg/ml)
0 1 3 6 9 0 1 3 6 9
AMPKα
P-AMPKα
AMPKβ
AMPKγ
Tubulin
HA
GFP
-70
-70
-35
-35
-55
-55
-25
B
Relative AMPKα protein
Time (h)
HA
HA-Crbn
C
Relative P-AMPKα protein
D
Relative AMPKβ protein
E
Relative AMPKγ protein
F
Relative AMPKα mRNA
G
Relative AMPKβ mRNA
H
Relative AMPKγ mRNA

Figure 4

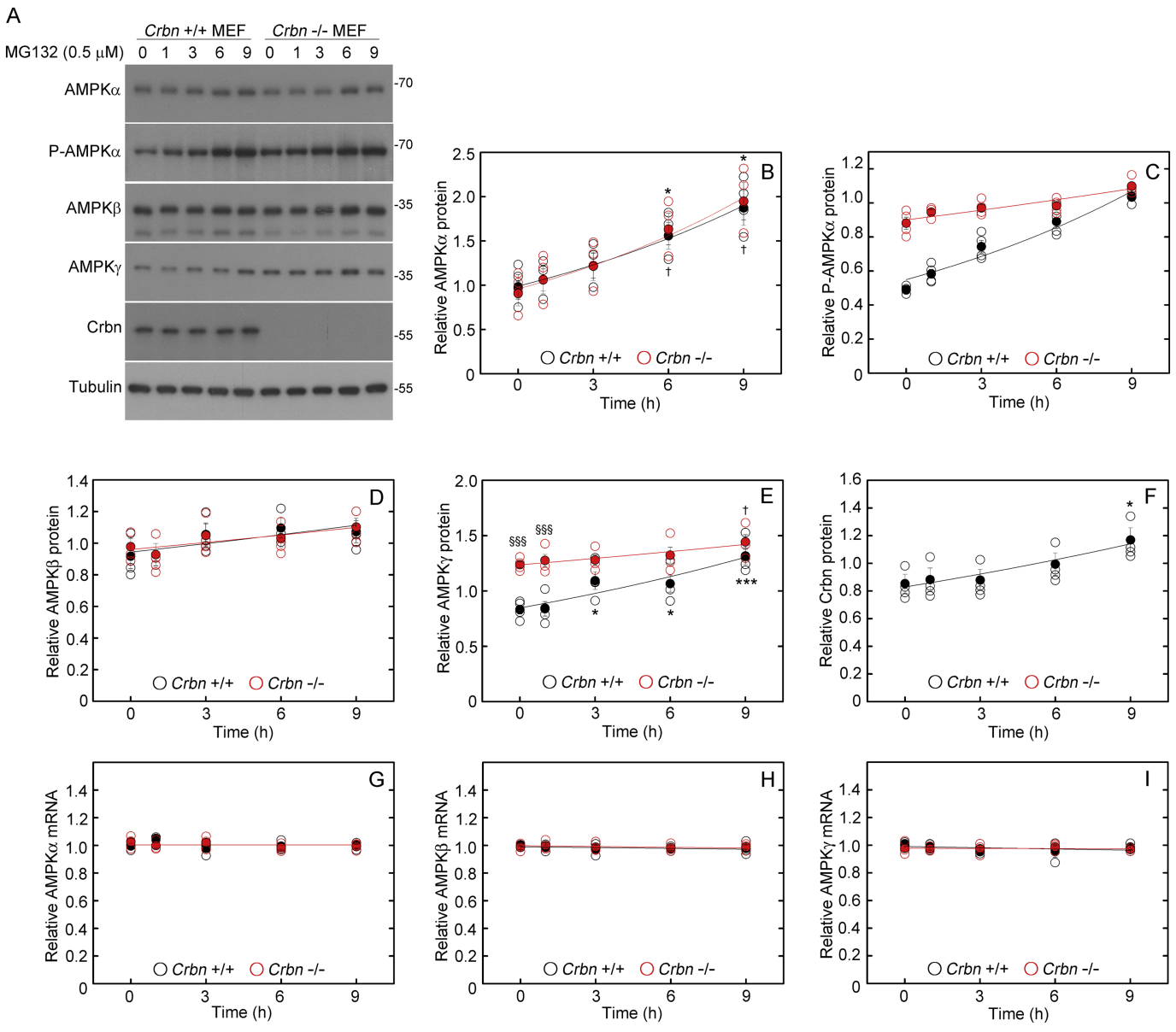
A
Crbn +/+ MEF
Crbn -/- MEF
MG132 (0.5 μM)
0 1 3 6 9 0 1 3 6 9
AMPKα
P-AMPKα
AMPKβ
AMPKγ
Crbn
Tubulin
-70
-70
-35
-35
-55
-55
B
Relative AMPKα protein
C
Relative P-AMPKα protein
D
Relative AMPKβ protein
E
Relative AMPKγ protein
F
Relative Crbn protein
G
Relative AMPKα mRNA
H
Relative AMPKβ mRNA
I
Relative AMPKγ mRNA
Crbn +/+
Crbn -/-
Time (h)

Figure 5

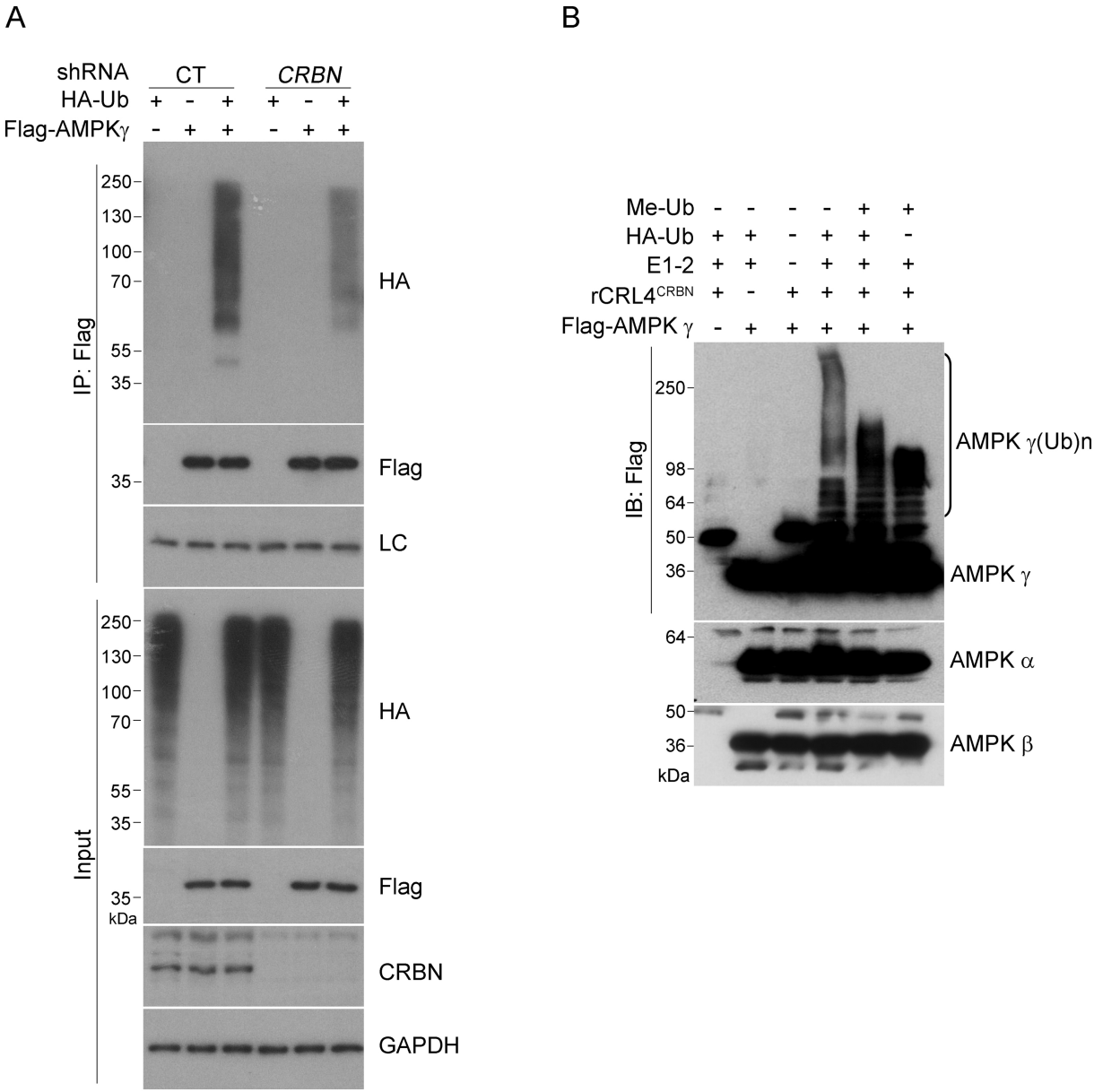
A
shRNA
CT
CRBN
HA-Ub
+ - + + - +
Flag-AMPKγ
- + + - + +
IP: Flag
250
130
100
70
55
35
HA
35
Flag
LC
Input
250
130
100
70
55
35
HA
35
kDa
Flag
CRBN
GAPDH
B
Me-Ub - - - - + +
HA-Ub + + - + + -
E1-2 + + - + + +
rCRL4CRBN + - + + + +
Flag-AMPK γ - + + + + +
IB: Flag
250
98
64
50
36
AMPK γ(Ub)n
AMPK γ
64
AMPK α
50
36
AMPK β
kDa

Figure 6